Indian J Phys (February 2021) 95(2):275–280
https://doi.org/10.1007/s12648-020-01696-5

ORIGINAL PAPER

Stoichiometry-related defect structure in lithium niobate and lithium tantalate

K Maaider[1,2]*, N Masaif[3] and A Khalil[2]

[1]Ecole Nationale des Sciences Appliquées, Univ. Sultan Moulay Slimane, B.P. 77, 25000 Khouribga, Marocco

[2]Laboratoire Rayonnement & Matière, E.R. Physique de la Matière et Modélisation, Univ. Hassan 1, B.P. 577, 26000 Settat, Marocco

[3]Département de Physique, Faculté des Sciences, Univ. Ibn Tofail, BP 133, 14000 Kénitra, Marocco

Received: 17 December 2018 / Accepted: 30 October 2019 / Published online: 5 March 2020

Abstract: Congruently grown $LiNbO_3$ ($LiTaO_3$) is known to be highly defective due to its significant Li_2O deficiency. We present in this work a comparative study between normal $LiNbO_3$ ($LiTaO_3$) and ilmenite structural $LiNbO_3$ ($LiTaO_3$). Namely, the normal cation stacking sequence is replaced by ilmenite ordering '…Nb (Ta) Li vacancy Li Nb (Ta) vacancy Nb (Ta) Li vacancy Li Nb (Ta) vacancy…'. From Safaryan's approach which combines a ferroelectric phase transition theory and vacancy models, we calculated the Curie temperature in ilmenite $LiNbO_3$ ($LiTaO_3$). We have shown that ilmenite structural $LiNbO_3$ ($LiTaO_3$) is in excellent agreement with the result of the experiment compared to normal $LiNbO_3$ ($LiTaO_3$).

Keywords: Ferroelectrics; Lithium niobate; Lithium tantalate; Defect structure; Vacancy models; Curie temperature

PACS Nos.: 61.72.-y; 61.72.jd; 74.62.Dh; 77.80.B

1. Introduction

$LiNbO_3$ and $LiTaO_3$ are two well-known ferroelectrics which possess among the highest spontaneous polarizations of all ferroelectrics. They have been the subject of intense study due to their many applications in the electro-optical, optical and piezoelectric fields. These materials that show a ferroelectric behavior are well known to be narrow-range nonstoichiometric compounds. In $LiTaO_3$, the solid solubility range extends from about 46–50.4 mol% of Li_2O at room temperature [1]. The structure of ferroelectric $LiTaO_3$ and that of $LiNbO_3$ belong to space group R3c and can be considered as a superstructure of the α-Al_2O_3 corundum structure with Li^+ and Ta^{5+} cations along the *c*-axis [2]. Recently, several workers have investigated the growing of high-quality single crystals of stoichiometric $LiTaO_3$ and $LiNbO_3$ which exhibit considerably wide nonstoichiometry at high temperature. Using the chemical bond method, a comprehensive description of the defect and the chemical bonding structure has been proposed by Xue et al. [3, 4].

To find which defect is involved in this phenomenon, we have proposed a theoretical description of the defect structure in $LiTaO_3$ and $LibO_3$ on the basis of a set of vacancy models combined with a ferroelectric phase transition theory. As $LiTaO_3$ is isomorphous with $LiNbO_3$, several defect models have been proposed for $LiNbO_3$.

Fay et al. [5] describe a ceramic sample assumed containing oxygen and lithium vacancies by the oxygen vacancy model having a formula $[Li_{1-2x}V_{2x}][Nb][O_{3-x}V_x]$ where [Li] represents the sublattice and V denotes the vacancies. This model cannot describe the density variation in function of the composition. In order to correct this anomaly, Lerner et al. [6] have predicted that an excess of niobium ions might occupy the lithium sites. This is the lithium vacancy model, which is given by the formula $[Li_{1-5x}Nb_xV_{4x}][Nb]O_3$ where the lithium vacancies are introduced taking into account the charge compensation. However, Peterson and Carnevale [7] observed a new defect structure corresponding to the Nb-site vacancy type using the NMR technique. Then, their niobium vacancy model is arranged as follows: $[Li_{1-5x}Nb_{5x}][Nb_{1-4x}V_{4x}]O_3$. Contrarily to the result pointed out by Abrahams and Marsh [8], Donnerberg et al. [9] proved that the niobium

*Corresponding author, E-mail: maaiderr@gmail.com

vacancy model is unfavorable to compare the energetic aspect of the defect structure models. A comparative study between the densities of these models allows Iyi et al. [10] to reject the oxygen vacancy model.

A theory of ferroelectric's phase transition in the crystal $LiNbO_3$ has been performed to understand and predict the properties of this crystal [11]. In this system, the solution of the dynamic problem of the crystal planes system exhibits the existence of the "soft mode" at the ferroelectric's transition.

For example, this method has been applied to the defect structure analysis of the lithium niobium single crystals [12] and lithium tantalate [13]. These studies provide a useful understanding of the phase transition dynamic behavior and the normal defect structure of $LiBO_3$ (B = Nb, Ta) [14].

Abdi et al. presented a complete model of the structure of intrinsic defects in $LiNbO_3$, based on Raman spectroscopy results. It is based on the coexistence of lithium (VLi) and niobium (VNb) vacancies. The reliability of this model and the associated calculations were verified by analyzing the frequencies and depreciation phonon modes, reinforced by Raman scattering measurements recorded in crystals of various compositions. They show that the Li vacancy is dominant in the structure of defects incongruent crystals [15].

The main aim of the present work is to investigate the defect structure in ilmenite-type lithium niobate and lithium tantalate and give a comparison between normal and ilmenite-type $LiBO_3$ (B = Nb or Ta).

Several experimental and theoretical studies have been developed on this subject and are mentioned in [9, 16, 17]. For example, in the work of Kong et al. [18], a weak peak at about 738 cm^{-1} reported as a very strong Raman peak of ilmenite phase $LiNbO_3$ was observed for nonstoichiometric $LiNbO_3$ crystals. However, Kumada et al. [17] have prepared the ilmenite-type structural $LiNbO_3$ by the ion exchange reaction in the molten salt $NaNbO_3$. Above a threshold temperature (500 °C), the structure of this new compound changes from the ilmenite to the $LiNbO_3$ type.

These results pushed us to propose a theoretical approach to study the defect structures of ilmenite-type $LiBO_3$ (B = Nb or Ta). This will allow us to give a comparison between the calculated normal and ilmenite values and the experimental data of the Curie temperature for the three vacancy models.

In this work, we present a description of the theoretical approach to study the Curie temperature of normal and ilmenite-type $LiBO_3$ (B = Ta, Nb) [14]. A detailed comparison between calculated values of the normal and ilmenite-type $LiBO_3$ and the experimental data of the Curie temperature is proposed in this paper.

2. Theoretical approach

2.1. The ilmenite structure

In the past, different models have been proposed in order to describe the accommodation of Li_2O deficiency in $LiNbO_3$. In what follows, we may omit the discussion of the model related to oxygen vacancies [5]. This contradicts the observed density changes upon increasing the nonstoichiometric. The two remaining models consider all compensating defects to occur on the cationic sublattices:

$$'LiNbO_3' \rightarrow 3Li_2O + Nb_{Li}^{4\bullet} + 4V_{Li}^{I} - LiNbO_3 \quad (1)$$

$$'LiNbO_3' \rightarrow 3Li_2O + 5Nb_{Li}^{4\bullet} + 4V_{Nb}^{5I} - LiNbO_3. \quad (2)$$

Donnerberg [19] has used Kroger–Vink notation [20] to formulate these chemical solid-state reactions. In addition, $LiNbO_3$ denotes the whole bulk of perfectly grown $LiNbO_3$. Model (1) corresponds to the chemical sum formula $Li_{1-4x}Nb_{1+x}O_3$, and model (2) to $(Li_{1-5x}Nb_{5x})Nb_{1-4x}O_3$.

The most obvious difference between reactions (1) and (2) relates to the concentration of niobium antisite defects ($Nb_{Li}^{4\bullet}$) and to the occurrence of Li or Nb vacancies.

In order to satisfy the experimental results of Abrahams and Marsh [8], Smyth [21] proposed the formation of appropriate defect clusters. Starting with the reaction

$$'LiNbO_3' \rightarrow 3Li_2O + Nb_{Li}^{4\bullet} + 4(Nb_{Li}^{4\bullet}V_{Nb}^{5I}) - LiNbO_3, \quad (3)$$

which immediately follows from Eq. (2) by a few re-arrangements, Smyth observed that the defect complexes $4(Nb_{Li}^{4\bullet}V_{Nb}^{5I})$ may be interpreted as basic Li vacancies within ilmenite-structured $LiNbO_3$, because perfect and ilmenite-structured $LiNbO_3$ differs only by their cation stacking sequence along the crystallographic c-axis, i.e.,

…BLi□BLi□BLi□BLi□BLi… perfect model
…BLi□LiB□BLi□LiB□BLi… Ilmenite model

Respectively, in this representation □ denotes a structural cation vacancy. The Li vacancies would be related to the LiB units. A necessary condition of this model to become favorable is that perfectly grown $LiBO_3$ and the ilmenite structure $LiBO_3$ are energetically almost equivalent.

In this work, we suppose that the ceramic samples of ilmenite-structured $LiBO_3$ (B = Ta or Nb) consist of single crystal on the basis of their structure. Such an assumption is based on the experimental fact that the ferroelectric phase transition occurred in the ceramic samples which are formed by parallel planes along the polar "*c*" axis. The projection of an elementary cell of ilmenite-type $LiBO_3$ on a plane, where the polar axis c lies, is shown in Fig. 1.

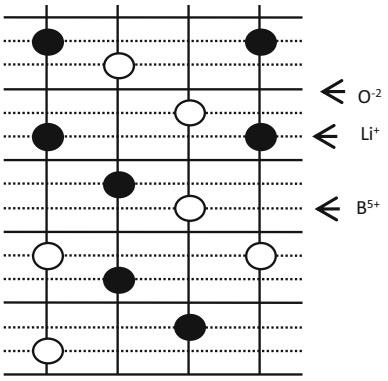

Fig. 1 Different planes in an elementary cell of crystal ilmenite $LiBO_3$

2.2. Soft mode frequency and Curie temperature

The new approach proposed by Safaryan [11] on ferroelectric transition in the crystal $LiNbO_3$ as well as by Masaif [13] on ferroelectric transition in the $LiTaO_3$ is tested from new results in order to discuss the main role of the nonstoichiometric compositions in the ilmenite-structured $LiBO_3$ compounds.

This approach [11, 12] manifests itself as a new tool to describe the defect structure mechanism in the ilmenite of lithium tantalate and lithium niobate where several physical quantities are relatively sensitive to the nonstoichiometric composition. For this purpose, it was necessary to initially find the part of the potential energy of interaction between the electrically charged planes. This interaction is responsible for the restoring force against the relative movement of the planes around their equilibrium positions.

The energy of the electrostatic interaction of two charged long lines is:

$$W = e^2\delta_i\delta_j b^2 \ln\frac{2l}{R_{ij}} \tag{4}$$

where $\delta_i = \frac{N_i q_i}{lb}$ with l, R_{ij}, q_i and N_i are the line length, the distance between the lines, the charge of ions and their number, respectively. We consider also the energy of repulsion between planes that can be put in the form B_{ij}/R_{ij}^n where n is large (6–10 for ionic crystals). We deduce the full energy of interaction of planes such as:

$$U_{ij} = -\frac{e^2 q_i q_j}{b}\ln\frac{2l}{R_{ij}} + \frac{B_{ij}}{R_{ij}^n} \tag{5}$$

Differentiating (5) for R_{ij}, we find the interaction force between planes. From the equilibrium condition ($U'_{ij} = 0$), we find the coefficient B_{ij},

$$B_{ij} = \frac{e^2 q_i q_j}{b\,n}(R_{ij}^0)^n \tag{6}$$

where R_{ij}^0 is the equilibrium distance between planes. Substituting (6) in (5), we can then expand the potential energy in terms of plane displacements from equilibrium positions $x_{ij} = R_{ij} - R_{ij}^0$. For U_{ij}, we receive up to the second order

$$U_{ij} = \frac{e^2 q_i q_j}{b}\left(\frac{1}{n} - \ln\frac{2l}{R_{ij}^0}\right) + \frac{e^2 q_i q_j n}{b\,(R_{ij}^0)^2}\frac{x_{ij}^2}{2} \tag{7}$$

The coefficient $C_{ij} = \frac{e^2 q_i q_j}{b\,(R_{ij}^0)^2}n$ describes the interaction between Li and O planes (as well as for Ta and O).

However, the interaction between Li and Ta (Nb) will deduce from the total energy:

$$U_{ij} = \frac{e^2 q_i q_j}{b}\ln\frac{2l}{R_{ij}^0} - \frac{B_{ij}}{R_{ij}} \tag{8}$$

Finally, for $LiBO_3$ crystal C_{ij} coefficients are

$$C_{ij} = \frac{e^2 q_i q_j}{b\,(R_{ij}^0)^2}n \tag{9}$$

Having the energy of interaction of planes per ion (5), Safaryan [11] and Masaif [13] reduced the dynamic problem of vibration of the system of charged planes to a problem of vibration of linear lattice, the unit cell of which (with parameter a) has three particles: Li^{1+}, B^{5+} and $3O^{2-}$. Let us denote the displacements of these particles in the sth unit cell through μ_s, ν_s and χ_s correspondingly (Fig. 2-a).

To solve the dynamic problem, we reduced the ilmenite type of the charged planes to a system of vibration of linear lattice (Fig. 2-b).

with $a = a' + a''$

In the lattice of equilibrate structure: a'

$$C_{\mathrm{Li-O}} \equiv C_{20} = -3\frac{q_0 q_2 e^2}{b\,R_{20}^2}n, \tag{10}$$

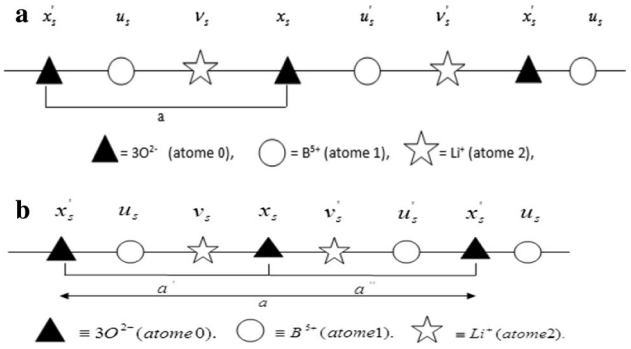

Fig. 2 **(a)** Linear lattice of ions Li^+, B^{5+} and triangle of ions O^{2-} replacing the system of crystal planes. **(b)** Displacement of Li^+, B^{5+} and $3O^{2-}$ ions in a linear lattice of the ilmenite type

$$C_{\mathrm{B-O}} \equiv C_{10} = -3\frac{q_0 q_1 e^2}{b R_{10}^2} n, \tag{11}$$

and

$$C_{\mathrm{Li-B}} \equiv C_{21} = \frac{q_1 q_2 e^2}{b R_{21}^2} n. \tag{12}$$

where q_1, q_2 and q_0 are, respectively, the electric charges of B^{5+}, Li^{+} and O^{2-} ions.In the lattice of the disordered structure: a''

$$C'_{\mathrm{Li-O}} \equiv C'_{20} = -3\frac{q_0 q_2 e^2}{b R'_{20}} n, \tag{13}$$

$$C'_{\mathrm{B-O}} \equiv C'_{10} = -3\frac{q_0 q_1 e^2}{b R'^2_{10}} n, \tag{14}$$

and

$$C'_{\mathrm{Li-B}} \equiv C'_{21} = \frac{q_1 q_2 e^2}{b R'^2_{21}} n. \tag{15}$$

In the study of ilmenite structure, we observe that the unstable part a' is defined by: BLiO. We must seek to find points of equilibrium between these ions, where R'_{ij} are the distances between separated ions.

The displacements of the three ions are indicated by v_s (Li^{+}), u_s (B^{5+}) and χ_s (O^{2-}). Then, the system is described by the differential equations as

$$\begin{aligned}
&(2M_2\omega^2 - C_{12} - C_{02} - C'_{12} - C'_{02})u + (C'_{12} + C_{12})v + (C_{02} + C'_{02})x = 0\\
&(C_{01} + C'_{12})u + (2M_1\omega^2 - C_{12} - C_{01} - C'_{12} - C'_{01})v + (C_{12} + C'_{01})x = 0\\
&(C_{02} + C'_{02})u + (C_{01} + C'_{01})v + (2M_0\omega^2 - C_{01} - C'_{01} - C_{02} - C'_{02})x = 0
\end{aligned} \tag{16}$$

The determinant of Eq. (16) is written:

$$\begin{aligned}
\Delta = {} & M_0M_1M_2\omega^6 - [M_0M_1(C_{12} + C_{20}) + M_1M_2(C_{10} + C_{20})\\
& + M_0M_2(C_{12} + C_{10})]\omega^4\\
& + [(C_{10}C_{12} + C_{10}C_{20} + C_{12}C_{20})(M_0 + M_1 + M_2)]\omega^2
\end{aligned} \tag{17}$$

where M_1, M_2 and M_0 are, respectively, the masses of the elements B, Li and O. The choice of solutions in the form of plane waves

$$g_s = g\, e^{i(\omega t + a s k)} \quad \text{with } g = u, v \text{ or } \xi \tag{18}$$

leads to a system, of linear equations, which has a non-trivial solution.

In order to obtain the fundamental frequencies of the optical branches, we put $k = 0$ in the determinant equation ($\Delta = 0$). Then, we get the following equation:

$$\omega^4 + F\omega^2 + S = 0 \tag{19}$$

where

$$\begin{aligned}
F = {} & -\frac{C'_{01}}{2M_0} - \frac{C'_{02}}{2M_0} - \frac{C_{01}}{2M_0} - \frac{C_{02}}{2M_0} - \frac{C'_{01}}{2M_1} - \frac{C'_{12}}{2M_1} - \frac{C_{01}}{2M_1}\\
& - \frac{C_{12}}{2M_1} - \frac{C'_{02}}{2M_2} - \frac{C'_{12}}{2M_2} - \frac{C_{02}}{2M_2} - \frac{C_{12}}{2M_2}\\
S = {} & \left(\frac{1}{4M_0M_1} + \frac{1}{4M_0M_2} + \frac{1}{4M_1M_2}\right)I + \frac{1}{4M_0M_1}J\\
& + \frac{1}{4M_0M_2}K + \frac{1}{4M_1M_2}L
\end{aligned}$$

and

$$\begin{aligned}
I = {} & (C'_{01}C'_{02} + C'_{01}C'_{12} + C'_{02}C'_{12} + C_{02}C_{01} + C'_{01}C_{02}\\
& + C'_{12}C_{02} + C_{01}C_{02} + C'_{02}C_{12} + C_{12}C_{02} + C'_{12}C'_{01})\\
J = {} & (C^2_{01} + C'_{01}C_{01} + C_{02}C'_{12})\\
K = {} & (C'_{12}C_{01} + C_{01}C_{12} + C'_{01}C_{12})\\
L = {} & (C'_{01}C_{12} + C'_{12}C_{12} + C^2_{12})
\end{aligned}$$

The optical modes are given by

$$\omega^2 = -\frac{1}{2}F - \frac{1}{2}(F^2 + 4S)^{1/2} \tag{20}$$

$$\omega^2 = -\frac{1}{2}F + \frac{1}{2}(F^2 + 4S)^{1/2} \tag{21}$$

At 0°K, the soft mode frequency ω^2 is proportional to the Curie temperature T_c. Substituting ω^2 by expression (21), the following relation that allows calculating the Curie temperature is obtained:

$$T^*_c = \frac{F^* - \sqrt{F^{*2} + 4 \times S^*}}{F - \sqrt{F^2 + 4 \times S}} T_c \tag{22}$$

The element X represents the exactly stoichiometric compositions, and X^* is the nonstoichiometric composition. Formula (22) allows us to calculate the Curie temperature for the different models. This will permit a comparison between this data and the experimental values. However, we represent these models, described previously, in the following condensed form.

$[Li_{\alpha_1}B_{\alpha_2}\theta_{\alpha_3}][B_{\beta_1}\theta_{\beta_2}][O_{3\gamma_1}\theta_{\gamma_2}]$; and $K^* = g\,K$ with $K = M$, q and $g = \alpha$, β or γ. Here, α, β and γ allow identifying the three models as follows:

1. Oxygen vacancy model corresponds to $\alpha_1 = 1 - 2x$, $\alpha_3 = 2x$, $\beta_1 = 1$, $\gamma_1 = 1\text{-}x/3$ and $\gamma_2 = x$; and $K^*_2 = \alpha_1 K_2, K^*_1 = \beta_1 K_1$ and $K^*_0 = \gamma_1 K_0$.
2. Tantalate or niobate vacancy model corresponds to $\alpha_1 = 1 - 5x$, $\alpha_2 = 5x$, $\beta_1 = 1 - 4x$, $\beta_2 = 4x$ and $\gamma_1 = 1$; and $K^*_2 = \alpha_1 K_2 + \alpha_2 K_1, K^*_1 = \beta_1 K_1$ and $K^*_0 = \gamma_1 K_0$.
3. Lithium vacancy model corresponds to $\alpha_1 = 1\text{–}5x$, $\alpha_2 = x$, $\alpha_3 = 4x$, $\beta_1 = 1$ and $\gamma_1 = 1$; and $K^*_2 = \alpha_1 K_2 + \alpha_2 K_1, K^*_1 = \beta_1 K_1$ and $K^*_0 = \gamma_1 K_0$.

In this representation, $\alpha = \beta = \gamma = 0$ means that ions and vacancies are absent in these nonstoichiometric models. The oxygen vacancy model is constructed taking into account the charge compensation for ilmenite structure in the nonstoichiometric $LiBO_3$ by the oxygen and the lithium vacancies. However, the tantalate (or niobate) vacancy model is arranged so that the vacancy does not exist in the Li site but in the Ta (or Nb) site.

In order to provide an adequate description of the defect ilmenite structure in nonstoichiometric $LiBO_3$, we have analytically performed the calculations of different physical quantities which are illustrated in Table 1. Estimates of T_c^* for Li (Ta or Nb) O_3 have been obtained by using the following values of the charges and the masses of ions: $q_O = q_0 = 2$, $q_{Ta} = q_{Nb} = q_1 = 5$, $q_{Li} = q_2 = 1$, $M_O = M_0 = 48$, $M_{Ta} = M_1 = 180.95$ (or $M_{Nb} = M_1 = 92.9$), $M_{Li} = M_2 = 6.94$.

3. Results and discussion

In principle, we could test these vacancy models by comparing the experimental results with the calculated values according to the theoretical approach previously mentioned. To make the comparison between the three vacancy models, we have used the experimental data of the Curie temperatures and the crystal parameters measured by Bennani and Husson [22] and those used in the Safaryan work [12].

To calculate the Curie temperatures, we need to know the Curie temperature of the exact stoichiometry compositions. The average values of the estimations are $T_{cTa} = 934$ K and $T_{cNb} = 1480$ K [14].

Comparing the experimental data with the theoretically calculated values, one can see a very close agreement between the measured temperatures and the lithium vacancy model values (Fig. 3). The obtained results show clearly that the Curie temperatures of the lithium vacancy model coincide with the experimental values. Consequently, this model shows that the Curie temperature decreases as the composition x increases. It is the first direct quantitative evidence that the lithium vacancies are indeed dominant in nonstoichiometric ilmenite $LiTaO_3$.

The oxygen and tantalate vacancies do not significantly contribute to the nonstoichiometry in these samples. Table 1 shows the measured Curie temperature and the calculated values of the ilmenite and normal nonstoichiometric $LiTaO_3$ for the lithium vacancy model (c).

To illustrate the defect ilmenite type of the nonstoichiometric $LiNbO_3$, we report in Fig. 4 the Curie temperature T_{cNb}^* as a function of the composition x. In this figure, we presented the defect structure vacancy models in the same x composition interval. Comparison between calculated values of (a), (b) and (c) models and experimental

Table 1 Comparison of phase transition temperatures in both normal [17] and ilmenite-type $LiTaO_3$

x	Measured	Normal	Ilmenite
0	917	919	919
0.005	906	874	876.873
0.008	861	850	849.17
0.02	783	764	768.559

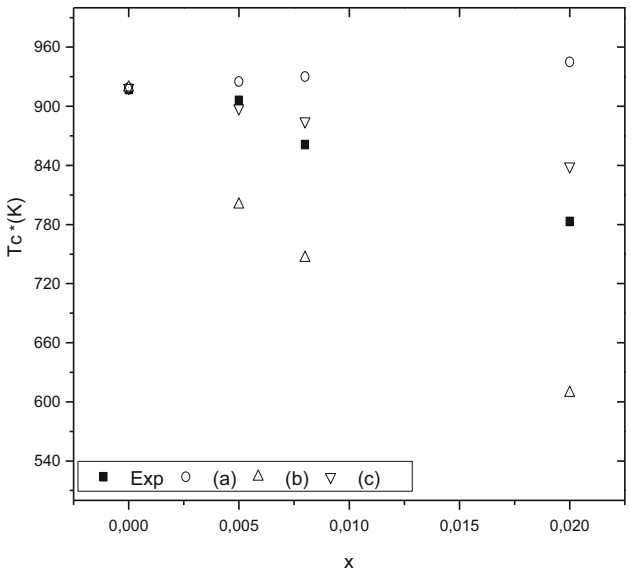

Fig. 3 Variation of the Curie temperature T_{cTa}^* of ilmenite versus nonstoichiometric composition x. The calculated values according to the (**a**), (**b**) and (**c**) vacancy models are compared to the experimental data of Ref. [17]

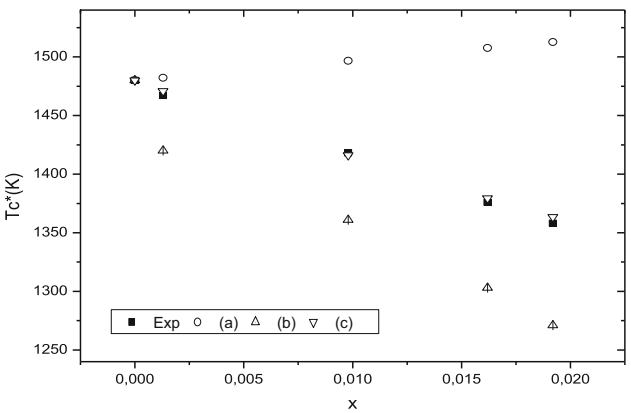

Fig. 4 Variation of the Curie temperature T_{cNb}^* of ilmenite versus nonstoichiometric composition x. The calculated values according to the (**a**), (**b**) and (**c**) vacancy models are compared to the experimental data of Ref. [10]

Table 2 Comparison of phase transition temperatures in both normal [9] and ilmenite-type $LiNbO_3$

x	Measured	Normal	Ilmenite
0.0013	1467	1469	1470.94
0.0098	1418	1404	1416.21
0.0162	1376	1358	1379.53
0.0192	1358	1338	1363.51

Table 3 The Curie temperature T^*_{cB} as a function of the nonstoichiometric composition x of the normal and ilmenite-type $LiBO_3$

	Ilmenite-type $LiBO_3$	Normal $LiBO_3$
T^*_{cTa}	$T^*_c = \frac{(1+7.69x)}{(1+20.07x)} T_c$	$T^*_c = \frac{1+0,62x}{1+10,86x} T_c$
$T^*_{c\,Nb}$	$T^*_c = \frac{(1+3.63x)}{(1+8.39x)} T_c$	$T^*_c = \frac{1+0,39x}{1+5.95x} T_c$

data is indicated in Fig. 4. As $LiNbO_3$ is isomorphous with $LiTaO_3$, we can deduce that the experimental Curie temperature is calculated from the lithium vacancy model, which confirms the previous results [23].

The measured Curie temperature and the calculated values of the ilmenite and normal nonstoichiometric $LiNbO_3$ for the lithium vacancy model (c) are shown in Table 2.

The analytical expressions of the Curie temperature of the normal and ilmenite-type $LiBO_3$ (Nb or Ta) are represented in Table 3.

The lithium vacancy model illustrated in Figs. 3 and 4 exhibits that the agreement between the experimental facts and theoretical predictions is quite satisfactory. The decrease in the Curie temperature can be interpreted in terms of competition between Li^+ and Ta^{5+} ions (Fig. 3), and between Li^+ and Nb^{5+} (Fig. 4). According to the (c) model, the linear increase with the increasing composition x results from an increasing Ta (or Nb) density and a decreasing Li density. The values of the lithium vacancy model are in excellent agreement with experimental data.

It is clear from Tables 1 and 2 that the results obtained by this theoretical approach show that the (c) model in ilmenite-type gives better results than in the normal structure. Furthermore, the ilmenite type is in better agreement than normal structure.

According to the experimental results used, we suggest that the ilmenite type is more dominant than the normal structure.

4. Conclusion

On the experimental measurements of Curie temperature, we have applied the theory of ferroelectric transition on the nonstoichiometric ilmenite-type $LiBO_3$ (B = Ta or Nb). This theoretical result proves the existence of ilmenite-like stacking defect in nonstoichiometric $LiBO_3$. The lithium vacancy model is quantitatively and qualitatively proved as the best model to interpret defect structure in lithium tantalate and lithium niobate. These results are in excellent agreement with the Li vacancy model and show us a new view on the intrinsic defect of $LiBO_3$.

Finally, this approach shows that the ilmenite-type structure is more probable to describe the experiment, particularly the mechanism responsible for substitution.

Acknowledgements We gratefully acknowledge financial support from the Ministry of Higher Education and the National Center for Scientific Research and Technology.

References

[1] M Paul, M Tabuchi and A R West *Chem. Mater*. **9** 3206 (1997)
[2] M E Lines and A M Glass, *Principles* (Oxford: Clarendon Press) (1977)
[3] X Zhang, D Xue and K Kitamura *Mater. Sci. Eng. B* **120** 21 (2005)
[4] X Zhang, D Xue and K Kitamura *Mater. Sci. Eng. B* **120** 27 (2005)
[5] H Fay, W J Alford and H M Dess *Appl. Phys. Lett*. **12** 89 (1968)
[6] P Lerner, C Legras and J P Dumas *J. Cryst. Growth* **3** 231 (1968)
[7] G E Peterson and A Carnevale *J. Chem. Phys.* **56** 4848 (1972)
[8] C S Abrahams and P Marsh *Acta Crystallogr. Sect. B* **42** 61 (1986)
[9] H Donnerberg, S M Tomlinson, C R A Catlow and O F Schirmer *Phys. Rev. B* **40** 11909 (1989)
[10] N Iyi, K Kitamura, F Izumi, J K Yamamoto, T Hayashi, H Asano and S Kimura *J. Solid State Chem.* **101** 340 (1992)
[11] F P Safaryan *Phys. Lett. A* **255** 191 (1999)
[12] F P Safaryan, R S Feigelson and A M Petrosyan *J. Appl. Phys.* **85** 8079 (1999)
[13] N Masaif, S Jebbari, F Bennani, A Jennane and M Hafid *Phys. Stat. Solidi (b)* **240** 640 (2003)
[14] K Maaider, A Jennane, A Khalil and N Masaif *Indian J. Phys.* **86** 575 (2012)
[15] F. Abdi, M.D. Fontana, M. Aillerie and P. Bourson. *J. Appl. Phys. A* **83** 427 (2006)
[16] S Yao, F Zheng, H Liu, J Wang, H Zhang, T Yan, J Wu, Z Xia and X Qin *Cryst. Res. Technol*. **44** 1235 (2009)
[17] N Kumada, N Ozawa, F Mut and N Kinomura *J. Solid. State Chem.* **57** 267 (1985)
[18] Y Kong, J Xu, X Chen, C Zhang, W Zhang and G Zhang *J. Appl. Phys.* **87** 4410 (2000)
[19] H Donnerberg *J. Solid State Chem.* **123** 208 (1996)
[20] F A Krôger and H J Vink *Point Defects in $LiNbO_3$*. (New York: Academic Press) (1986)
[21] D M Smyth *Proceedings of the sixth international symposium on application of ferroelectrics*. p 115 (1986)
[22] F Bennani, E Husson *J. Eur. Ceram. Soc.* **21** 847 (2001)
[23] X Zhang and F Xue *J. Phys. Chem. B* 111 **2587** (2007)